



Published in final edited form as:

Neuroimaging Clin N Am. 2014 November ; 24(4): 655–669. doi:10.1016/j.nic.2014.07.009.

Resting state BOLD fMRI for pre-surgical planning

Mudassar Kamran^a, Carl D Hacker^b, Monica G Allen^{a,c}, Timothy J Mitchell^{a,c}, Eric C Leuthardt^c, Abraham Z Snyder^{a,d}, and Joshua S Shimony^a

Mudassar Kamran: kamranm@mir.wustl.edu; Carl D Hacker: hackerc@wusm.wustl.edu; Monica G Allen: allenm@npg.wustl.edu; Timothy J Mitchell: mitchell@physics.wustl.edu; Eric C Leuthardt: leuthardte@wudosis.wustl.edu; Abraham Z Snyder: avi@npg.wustl.edu

^aMallinckrodt Institute of Radiology, Washington University School of Medicine, 4525 Scott Ave., Saint Louis, MO 63110 USA, Tel: 314-362-5949

^bMedical Student Training Program, Washington University School of Medicine, 4525 Scott Ave., Saint Louis, MO 63110 USA, Tel: 314-362-5949

^cDepartment of Neurological Surgery, Washington University School of Medicine, 4525 Scott Ave., Saint Louis, MO 63110 USA, Tel: 314-362-5949

^dDepartment of Neurology, Washington University School of Medicine, 4525 Scott Ave., Saint Louis, MO 63110 USA, Tel: 314-362-5949

SYNOPSIS

Resting state functional MRI (rsfMRI) measures spontaneous fluctuations in the BOLD signal and can be used to elucidate the brain's functional organization. It can be used to simultaneously assess multiple distributed resting state networks. Unlike task fMRI, rsfMRI does not require task performance and thus can be performed in any subject that can obtain an MRI scan. In this article we present a brief introduction of rsfMRI processing methods followed by a detailed discussion on the use of rsfMRI in pre-surgical planning. Example cases are provided to highlight the strengths and limitations of the technique.

Keywords

Functional MRI; Resting state functional MR imaging (rsfMRI); Resting State Networks (RSNs); Multi Layered Perception (MLP); Eloquent Cortex

1. Introduction

1.1. Background

Functional MRI (fMRI) detects changes in the blood oxygen level dependent (BOLD) signal that reflect the neurovascular response to neural activity. Traditionally, fMRI has been used

© 2014 Elsevier Inc. All rights reserved.

Corresponding Author: Joshua S Shimony: shimonyj@mir.wustl.edu.

Publisher's Disclaimer: This is a PDF file of an unedited manuscript that has been accepted for publication. As a service to our customers we are providing this early version of the manuscript. The manuscript will undergo copyediting, typesetting, and review of the resulting proof before it is published in its final citable form. Please note that during the production process errors may be discovered which could affect the content, and all legal disclaimers that apply to the journal pertain.

to localize function within the brain by presenting a stimulus or imposing a task (such as presenting a flashing checker board pattern or generating verbs from nouns) to elicit neuronal responses [1], [2]. This type of experiment has been very effective at localizing functionality within the brain, as evidenced by the many thousands of publications utilizing task based fMRI.

The human brain consumes a disproportionate amount of energy relative to its weight. The brain constitutes approximately 2% of the body's weight, but consumes 20% of the body's energy utilization [3]. Performance of a task only minimally increases energy expenditure [4]. Thus, task based experiments ignore the majority of the brain's activity, which is largely devoted to signaling [4]–[8].

Biswal and colleagues were the first to demonstrate that spontaneous fluctuations in the BOLD signal in the resting state correlated within the somatomotor system [9]. Prior to this observation, spontaneous fluctuations in the BOLD signal in the resting state were regarded as noise and generally averaged out over many trials or task blocks [10], [11]. More recent studies have shown that these spontaneous fluctuations reflect the brain's functional organization [12]. Correlated intrinsic activity currently is referred to as functional connectivity MRI or resting state fMRI (rsfMRI). The development of these methods has opened up many exciting possibilities for future neurocognitive research as well as clinical applications. This review focuses on the application of rsfMRI to presurgical planning. Table 1 summarizes key features of both task fMRI and rsfMRI. A historical review is given in [12].

1.2. Resting State Networks

Correlated intrinsic activity defines functional connectivity. Functionally connected regions are known as resting state networks (RSNs; equivalently, intrinsic connectivity networks [13]. The resting state fMRI scans generally are acquired while the subject is in a state of quiet wakefulness [14]. The importance of RSNs lies in the fact that their topography closely corresponds to the topography of responses elicited by a wide variety of sensory, motor, and cognitive tasks [15]. Intrinsic activity persists, albeit in somewhat modified form, during sleep [16], [17] or even under sedation [18]. The persistence of the spontaneous fluctuations during states of reduced awareness suggests that intrinsic neuronal activity plays an important role in the maintenance of the brain's functional integrity [19]. Spontaneous BOLD activity has been detected in all mammalian species investigated thus far [20]–[22], which reinforces the notion that this phenomenon is important from a physiological and evolutionary point of view. However, the precise physiological functions of intrinsic activity remain unknown. Examples of important RSNs follow and are summarized in Table 2.

1.2.1 Default Mode Network (DMN)—Perhaps the most fundamental RSN is the Default Mode Network (DMN) (Figure 1A), first identified by a meta-analysis of task-based functional neuroimaging experiments performed with positron emission tomography (PET) [23], [24]. The defining property of the DMN is that it is more active at rest than during performance of goal-directed tasks. The DMN was first identified using rsfMRI by Greicius et al. [25] a finding that has since been replicated many time over using a variety of analysis

methods [15], [26]–[32]. Some investigators have hypothesized that there are two large anti-correlated systems in the brain [33], [34], one anchored by the DMN and the other comprised of systems controlling executive and attentional mechanisms. This dichotomy has been variously referred to as “task-positive” vs. “task-negative [28], [32], [33], [35], [36] and “intrinsic” vs. “extrinsic” [34], [37]. Although the nomenclature associated with the DMN remains controversial [38], [39], the topography of the DMN is remarkably consistent across diverse analysis strategies.

1.2.2 Sensory and Motor RSN—The somatomotor (SMN) network, first identified by Biswal and colleagues [9], encompasses primary and higher order motor and sensory areas (Figure 1B). The visual (VIS) network spans much of the occipital cortex (Figure 1C) [15], [26]–[29]. The auditory network (AUD) includes Heschl’s gyrus, the superior temporal gyrus, and the posterior insula [15]. The language network (LAN) includes Broca’s and Wernicke’s areas but also extends to prefrontal, temporal, parietal, and subcortical regions (Figure 1D) [40]–[42].

1.2.3 Attention and Cognitive Control RSN—RSNs involved in attentional and cognitive control include the dorsal attention network (DAN) and the ventral attention network (VAN) [13], [28], [29], [43], [44]. The DAN (Figure 1E) includes the intraparietal sulcus and the frontal eye fields and is recruited by tasks requiring control of spatial attention. The ventral attention network (Figure 1F), which includes the temporal-parietal junction and ventral frontal cortex, is involved in the detection of environmentally salient events [43]–[45]. The frontoparietal control network (FPC) (Figure 1G), which includes the lateral prefrontal cortex and the inferior parietal lobule, is associated with working memory and control of goal-directed behavior [46], [47]. Finally, the cingulo-opercular network (CON), also known as the salience network [13] or the core control network [48] includes the medial superior frontal cortex, anterior insula, and anterior prefrontal cortex. The CON is thought to enable the performance of tasks requiring executive control [28], [47], [48].

2. Application to Pre-surgical Planning

2.1. Review of the Literature

Multiple studies have demonstrated that maximal resection of a brain tumor while sparing nearby eloquent cortex leads to improved outcomes with reduced morbidity [49]–[53]. Similar considerations apply to surgical resections for intractable epilepsy. Historically, neurosurgeons have been concerned with localization of the motor and language system since these parts of the brain instantiate critical functionality (“eloquent” cortex). However, a broader understanding of brain function suggests that all parts of the brain contribute to important functionality [29], [32], [34], [42]. Thus, improved functional mapping of multiple RSNs beyond motor and language systems could lead to further improvements in patient outcomes.

Several prior publications have explored the use of rsfMRI for use in pre-surgical planning. An early case report described use of rsfMRI to localize the motor cortex in a patient with a brain tumor [54]. Kokkonen et al. [55] similarly compared motor task fMRI data to resting state data and showed that the motor functional network could be localized on the basis of

resting state data in 8 tumor patients, as well as 10 healthy control subjects. In surgery for epilepsy, the higher spatial resolution afforded by rsfMRI over electroencephalography could provide a distinct advantage in mapping epileptic foci or networks. Seed-based methods were used by Liu et al. [56] to successfully locate sensorimotor areas by using rsfMRI in patients with tumors or epileptic foci close to sensorimotor areas. They found agreement between rsfMRI, task-based fMRI, as well as intraoperative cortical stimulation data. In another study from the same laboratory, Stufflebeam and colleagues [57] were able to localize areas of increased functional connectivity in 5 of 6 patients that overlapped with epileptogenic areas identified by invasive encephalography. Zhang et al. [58] used graph methods and a pattern classifier applied to rsfMRI data to identify subjects as either having medial temporal lobe epilepsy or as normal controls. Using data from 16 patients with intractable medial temporal lobe epilepsy and 52 normal controls, they achieved an average classification sensitivity of 77.2% and a specificity of 83.86%. Bettus et al. [59] reported that increases in basal functional connectivity were a specific marker of the location of the epileptogenic zone in 22 patients with mesial temporal lobe epilepsy. Weaver et al. [60] studied four non-lesion, focal epileptic patients along with 16 control subjects to determine whether the seizure focus could be found using the functional patterns near the epileptogenic zone. By averaging voxel homogeneity across regions of interest and comparing that with other regions, they were able to accurately identify the epileptic focus. Tie et al. [61] used spatial Independent Component Analysis (sICA) on a training group of 14 healthy subjects to identify the language network on the basis of rsfMRI. The result of that analysis was then used to identify the language network in a second group of 18 healthy subjects at the individual level. They further propose an automated system for localizing the language network in individual patients using sICA. A more detailed presentation of our experience using rsfMRI for pre-surgical mapping with both seed based and MLP approaches follows in the next sections.

2.2. Overview of Processing Methods

rsfMRI methodology currently is dominated by two complementary strategies, spatial Independent Components Analysis (sICA) [26] and seed-based correlation mapping [9]. Both strategies depend on the fact that spontaneous neural activity is correlated (phase coherent) within widely distributed regions of the brain. Both strategies yield highly reproducible results at the group level [30], [62]. sICA decomposes resting state fMRI data into a sum of components, each component corresponding to a spatial topography and a time course. In contrast, seed-based correlation mapping is computed by voxel-wise evaluation of the Pearson correlation between the time courses in a targeted region of interest (ROI) and all other voxels in the brain [63].

The principal advantage of sICA is that it provides a direct means of separating artifact from BOLD signals of neural origin, although this separation typically requires observer expertise. The results obtained using sICA may vary substantially depending on processing parameters (e.g., number of requested components). Thus, sICA can be difficult to use in the investigation of targeted RSNs, especially in single subjects. In contrast, targeting of selected RSNs is built-in to seed-based correlation mapping. However, the principal

difficulty in using seed-based correlation mapping is exclusion of non-neural artifact, which typically is accomplished using regression techniques [63]–[65].

sICA and seed-based correlation mapping both represent strategies for assigning RSN identities to brain voxels. Since sICA makes no a priori assumptions regarding the topography of the obtained components, this method exemplifies unsupervised classification. In contrast, seed-based correlation mapping depends on prior knowledge, and so exemplifies supervised classification. For additional discussion of the distinction between supervised vs. unsupervised methodologies see [42].

We recently described a technique for mapping the topography of known RSNs in individuals using a multilayer perceptron (MLP) [42]. Perceptrons are machine learning algorithms that can be trained to associate arbitrary input patterns with discrete output labels [66]. An MLP was trained to associate seed-based correlation maps with particular RSNs. Running the trained MLP on correlation maps corresponding to all voxels in the brain generates voxel-wise RSN membership estimates. Thus, RSN mapping using a trained MLP exemplifies supervised classification. An example of the RSN produced by the MLP algorithm in three subjects is presented in Figure 2.

In [42] it was demonstrated that the MLP accurately generates RSN topography estimates in individuals consistent with previous studies, even in brain regions not represented in the training data. These findings are important to future applications because they demonstrate that this approach can reliably and effectively map multiple RSNs in individual subjects.

2.3 Preoperative Sensorimotor Mapping in Brain Tumor Patients using seed based approach

Zhang et al. [67] describe our initial experience in using rsfMRI brain mapping for presurgical planning of tumor resections in four tumor patients. The tumors in all four patients were adjacent to the motor and sensory cortices, thus necessitating accurate localization prior to surgery to minimize post-operative deficits. Each of the patients was scanned using rsfMRI and again using task-based fMRI while performing a block design finger-tapping task. fMRI in each patient included four 7-minute runs (28 minutes total). rsfMRI data previously acquired from a group of normal controls (N=17) was also used for comparison.

In the tumor patients, the seed was placed in the hemisphere contralateral to the tumor at coordinates taken from an independent group of subjects that performed a button-press task [68], [69]. Electro-Cortical Stimulation Mapping (ECS) was performed on three of the four tumor patients, and these data, in addition to task based fMRI, was used for comparison with the resting state data. Compared with the task-based fMRI, the results of rsfMRI analysis were more consistent with the intraoperative ECS findings. Given that rsfMRI does not depend on task performance by the patient this outcome suggests that rsfMRI may be more reliable for purposes of presurgical planning.

We discuss two of the four patients from this manuscript:

Case 1: A glioblastoma was diagnosed in the right hemisphere of a 45 year old man. ECS during the surgery found that motor cortex was shifted anteriorly. Figure 3A shows the results of the task based fMRI, which confirmed the anterior displacement of motor cortex. However, the task-based result was unreliable, as one of the runs showed likely artifactual activation in the posterior part of the tumor (magenta arrow in Task 2). rsfMRI (Figure 3B) was more consistent and also demonstrated anterior shifting of motor cortex ipsilateral to the tumor.

Case 2: A 64-year-old man developed focal motor seizures secondary to mass in the left hemisphere (Figure 4A). Finger-tapping fMRI showed atypical response topography including activation in right parietal cortex in addition to the expected activation of the somatomotor area (Figure 4B). Seed-based (Figure 4C) correlation mapping rsfMRI showed the somatomotor RSN without parietal involvement. Correlation mapping with a seed in right parietal cortex matched the topography of the DAN (Figure 4D). Our interpretation of this result is that, during the task fMRI, the patient had to strongly focus his attention in order to complete the task, which accounts for the activation in the attentional network. This case illustrates the potential increased specificity of the rsfMRI method. The findings of the rsfMRI were consistent with the intraoperative ECS.

2.4 Preoperative Mapping of Functional Cortex using the Multi Layered Perception (MLP)

Mitchell and colleagues reported application of MLP-based RSN mapping to pre-surgical planning in 6 patients with intractable epilepsy and 7 patients with brain tumors [70]. Epilepsy patients underwent electrocorticographic monitoring to localize the epileptogenic zone of seizure onset and to perform functional mapping with ECS. Patients with tumors underwent intra-operative ECS mapping prior to resection of the tumor mass. In this review we focus only on the results in the epilepsy patients.

Pre-operative rsfMRI analysis—MLP analysis was performed in all patients as previously described. To determine the probability that an electrode covers a portion of a RSN, electrode MRI co-registration was used with the results of the MLP analysis, and gray matter voxels located within 30 mm of the electrode were averaged with a weight inversely proportional to the square of their distance from the electrode.

Electrode MRI co-registration in seizure monitoring patients—Electrodes were segmented on the basis of a CT image co-registered to the patient's MRI using methodology similar to that previously described [71], [72]. Electrodes imaged in the post-grid implantation CT typically are displaced inward relative to the cortical surface imaged on pre-operative MRI because of traction from dural over-sewing and post-surgical edema. This inward displacement was corrected by projecting electrode coordinates outwards to the brain surface along a path normal to the plane of the grid.

Electrocortical Stimulation Mapping—Electrodes were classified as over eloquent cortex using ECS mapping. Motor regions were defined by the presence of induced involuntary motor movements. Language sites were defined by speech arrest during stimulation.

Comparison of MLP-based RSN mapping to ECS mapping—An electrode was classified as positive or negative in the MLP results according to the probability of its belonging to the appropriate RSN (motor or language). These probabilities were then plotted against the ECS results to generate receiver-operator characteristic (ROC) curves. These ROC curves were averaged and the area under the averaged curve (AUC) was used as a measure of the agreement between the MLP vs. ECS methods.

Results in epilepsy patients—Figure 5 demonstrates a high degree of qualitative overlap between the location of the motor and language networks as compared to the ECS results in the epilepsy patients. The positive motor ECS electrodes were centered in the pre-central gyrus. The MLP-mapped motor areas encompassed both the pre- and post-central gyri. The positive language ECS electrodes were centered in the pars opercularis of the inferior frontal gyrus (IFG), approximately in Brodmann area (BA) 44. The MLP language positive regions were in pars triangularis of the IFG, which corresponds to BA 45. The anteriorly shifted MLP-based localization of language cortex (BA 45 vs. 44) demonstrates expected differences between the two methods related to methodology and suggests the possibility that the definition of eloquent cortex should be expanded. Quantitative comparisons were performed with an ROC analysis which yielded an average area under the curve (AUC) of 0.89 for the motor network and an average AUC of 0.76 for the language network. These findings demonstrate that MLP-based mapping can identify RSNs in the presence of distorted anatomy.

Minimization of false negatives—Loci in MLP maps outside the appropriate RSN but eloquent as determined by ECS are defined as MLP false negatives. Minimization of MLP false negatives is critical to reduce surgical morbidity, since resection of a false negative area could lead to a clinical deficit. Figure 6 illustrates the results of an analysis undertaken to minimize MLP motor false negatives. This analysis showed that the probability of a MLP false negative could be reduced to less than 2% by expanding the “no-cut” zone by 15mm around the contour corresponding to 85% likelihood of belonging to the motor RSN.

In summary, MLP-based RSN mapping robustly identified all networks in all patients, including those with distorted anatomy attributable to mass effect. When the ECS positive sites were analyzed, rsfMRI had AUCs of 0.89 and 0.76 for motor and language identification, respectively. MLP false negatives were minimized by including a 15 mm safety margin around the edge of the motor RSN. These findings demonstrate that the MLP-defined RSNs are able to identify eloquent cortex.

A summary of key points in regard to the application of rsfMRI in pre-surgical planning is presented in Table 3. Herein, we present example cases that illustrate the integration of resting state functional MR imaging in neurosurgical planning for patients with brain tumors, particularly when the application of ECS may be limited.

2.5 Illustrative cases

2.5.1 Case example 1—A 57 year-old-man with distant history of rectal adenocarcinoma presented with persistent headache and blurred vision. Brain MRI examination demonstrated

an enhancing left frontoparietal mass, initially favored to represent a high grade primary glial neoplasm.

Preoperative resting state fMR imaging showed the left motor activation center was located anterior superior to the tumor, abutting the peri-tumor edema with minimal displacement (Figure 7A). Broca's area was located anterior to the peri tumor edema, while Wernicke's area abutted the inferior portion of left frontoparietal junction mass (Figure 7B). Given the close proximity of the mass to the motor and language centers it was decided that an awake-craniotomy would be performed with ECS.

In the operating room, following administration of the circumferential field block the patient was noted to have significant aspiration, with the gastric contents appearing at the patient's nose and mouth. Proceeding with an awake-craniotomy and brain mapping were felt to be of considerable risk given the aspiration. Surgical options at this stage included: (a) to perform a biopsy alone or (b) proceed with surgical resection based on the preoperative fMRI that would offer therapeutic benefit, however at an increased risk of permanent speech or motor deficits. After consultation with the family it was decided to continue with surgical resection given the preoperative resting state fMR imaging findings that helped characterize the spatial relationship between the motor and language centers and the frontoparietal mass, suggesting a potential corridor through the parietal lobe for tumor resection.

A standard craniotomy was then performed. Continued stereotactic navigation was used to visualize the optimal gyrus for surgical approach. This surgical corridor was posterior and oblique relative to the tumor and non-intuitive on the basis of anatomy landmarks alone. Along this deeper track the tumor was gross totally resected. This resection of the tumor was confirmed with intraoperative MR imaging.

The patient's post-operative course was unremarkable with no new speech or motor deficits. Surgical pathology results were consistent with glioblastoma multiforme, WHO grade 4. Following the frontoparietal tumor resection, the patient experienced complete resolution of headache and blurred vision.

2.5.2 Case example 2—A 47 year-old man with left frontal lobe anaplastic oligodendroglioma undergoing chemotherapy treatment, status post partial surgical resection and post fractionated radiation treatment, was noted to have a new mass-like nodular area of enhancement at the tumor resection site on the one-year follow up brain MRI examination. These imaging findings were concerning for tumor recurrence. The patient had profound expressive aphasia at the time of presentation and thus could not perform task fMRI.

Resting state fMRI demonstrated regions related to motor (Figure 7C) and Wernicke's area were not in close proximity to the recurrent tumor and were therefore of less concern from a neurosurgical standpoint. However, Broca's area was less than 1 cm from the edge of the previous resection cavity and abutting the edematous parenchyma surrounding the new foci of enhancement (Figure 7D).

Consensus decision on the basis of the clinical picture and the imaging findings was to perform a repeat awake-craniotomy with surgical resection of the recurrent tumor. This was

discussed with the patient. A standard awake craniotomy was performed; however, once the brain was exposed and the patient was roused, the patient was combative and could not adequately follow the commands despite repeated attempts of mild sedation using narcotics to reduce the patient's pain and discomfort. Given the patient's condition, mapping could not be accomplished. A 2×2 cm block of tissue corresponding to the enhancing mass noted on the prior MRI examination was resected, furthest away from the speech and motor areas identified on preoperative rsfMRI.

Postoperatively, there was no worsening of patient's speech or motor function. Biopsy results for the resected tissue were consistent with radiation necrosis with no evidence of tumor recurrence.

2.5.3 Case example 3—A 41-year-old man with a history of grade III anaplastic astrocytoma, status post awake-craniotomy, was noted to have a new enhancing lesion in the superior temporal gyrus on routine follow up brain MRI examination, three years after the initial surgery.

Pre-operative rsfMRI demonstrated a distinct gap between the site of recurrence and the language network. Wernicke's area localized 2 cm posterior to the recurrent tumor. Given concern for recurrence, the patient was considered for minimally invasive laser ablation treatment. The alternative of a standard awake craniotomy with brain mapping and surgical resection was discussed. However the patient chose the less invasive laser ablation treatment, which was believed to be optimal given the confidence in the preoperative resting state fMRI findings. The laser interstitial thermal ablation involves the stereotactic placement of a laser probe into the tumor for MRI guided heating of the lesion.

Preoperatively, the planned trajectory took into account the resting state networks for language thus allowing successful penetration of the tumor, without disrupting language associated sites.

The patient's postoperative course was unremarkable and he was discharged from the hospital two days following the minimally invasive laser ablation treatment without complications.

2.5.4 Case example 4—A 29-year-old multilingual man developed grade IV Glioblastoma Multiforme, status post biopsy and chemo-radiation treatment. On the most recent one-year follow-up MR examination, a new focus of enhancement was identified in the white matter of the left frontal lobe.

The preoperative rsfMRI showed close proximity between the suspected tumor recurrence and the language network, with the tumor located deep to the activation corresponding to Broca's area. The new focus of enhancement was located several centimeters anterior to the motor strip, and less than a centimeter distant from the supplementary motor area. Given these findings, awake-craniotomy and resection of tumor was planned.

During the awake-craniotomy, once the brain was exposed, stereotactic navigation was used to localize the site of the recurrent tumor. Electro-cortical stimulation mapping was

performed at the tumor site and adjacent regions with multiple iterations using various speech paradigms, with no speech arrest. Of note these negative sites included regions identified with task and resting state fMRI as belonging to the language network. Subsequently, sub-pial dissection and resection of the inferior frontal gyrus affected by the tumor was performed, while the patient was maintained in conversation without any difficulty.

During the post-operative hospital stay and at the time of discharge, the patient's sensory and motor components of speech did not demonstrate any worsening. Contrary to illustrative case numbers 1–3, this example illustrates that the resting state functional MR imaging, though useful for operative planning should be used in conjunction with ECS when possible, since it remains the gold standard technique for functional mapping of the brain during neurosurgery.

4. Conclusion

This article provides a brief overview of rsfMRI and its applications in neurosurgical practice. We briefly discussed the RSN imaging methods and the common analysis techniques with limited literature review. Finally, we presented several cases from our experience using the MLP-based technique in patients with brain tumors. This experience suggests how MLP-based RSN mapping can be applied to assist in pre-surgical planning.

As these results demonstrate, rsfMRI is a promising technique for pre-surgical planning with the objective of decreasing morbidity while maximizing complete resection of pathological tissue. However, the methodology is still in early stages of development. Further research is necessary to make these tools more accurate and available in the operating room. Additional research is needed to explore the differences between rsfMRI and ECS mapping, and to better understand the consequences of disrupted RSNs outside the motor and language systems. Related engineering development should incorporate the pre-surgical MRI results into intra-operative neuro-navigation systems, including the rsfMRI results in conjunction with white matter fiber bundle anatomy derived from diffusion tensor imaging.

Acknowledgments

We wish to thank the National Institute of Health for its generous support of this project via NIH R21 CA159470. Dr. Snyder is supported by NIMH Grant P30 NS048056.

References

1. Posner, MI.; Raichle, ME. Images of mind. New York: Scientific American Library; Distributed by W.H. Freeman and Co; 1997.
2. Spitzer M, Kwong KK, Kennedy W, Rosen BR, Belliveau JW. Category-specific brain activation in fMRI during picture naming. *Neuroreport*. Nov; 1995 6(16):2109–2112. [PubMed: 8595181]
3. Clarke, DD.; Sokoloff, L. [Accessed: 08-Apr-2014] Circulation and Energy Metabolism of the Brain. 1999. [Online]. Available: <http://www.ncbi.nlm.nih.gov/books/NBK20413/>
4. Raichle ME, Mintun MA. Brain Work and Brain Imaging. *Annu Rev Neurosci*. 2006; 29(1):449–476. [PubMed: 16776593]

5. Shulman RG, Rothman DL, Behar KL, Hyder F. Energetic basis of brain activity: implications for neuroimaging. *Trends Neurosci.* Aug; 2004 27(8):489–495. [PubMed: 15271497]
6. Attwell D, Laughlin SB. An Energy Budget for Signaling in the Grey Matter of the Brain. *J Cereb Blood Flow Metab.* Oct; 2001 21(10):1133–1145. [PubMed: 11598490]
7. Ames A 3rd, Li YY, Heher EC, Kimble CR. Energy metabolism of rabbit retina as related to function: high cost of Na⁺ transport. *J Neurosci Off J Soc Neurosci.* Mar; 1992 12(3):840–853.
8. Lennie P. The cost of cortical computation. *Curr Biol CB.* Mar; 2003 13(6):493–497.
9. Biswal B, Yetkin FZ, Haughton VM, Hyde JS. Functional connectivity in the motor cortex of resting human brain using echo-planar MRI. *Magn Reson Med Off J Soc Magn Reson Med Soc Magn Reson Med.* Oct; 1995 34(4):537–541.
10. Purdon PL, Weisskoff RM. Effect of temporal autocorrelation due to physiological noise and stimulus paradigm on voxel-level false-positive rates in fMRI. *Hum Brain Mapp.* 1998; 6(4):239–249. [PubMed: 9704263]
11. Triantafyllou C, Hoge RD, Krueger G, Wiggins CJ, Potthast A, Wiggins GC, Wald LL. Comparison of physiological noise at 1.5 T, 3 T and 7 T and optimization of fMRI acquisition parameters. *NeuroImage.* May; 2005 26(1):243–250. [PubMed: 15862224]
12. Snyder AZ, Raichle ME. A brief history of the resting state: the Washington University perspective. *NeuroImage.* Aug; 2012 62(2):902–910. [PubMed: 22266172]
13. Seeley WW, Menon V, Schatzberg AF, Keller J, Glover GH, Kenna H, Reiss AL, Greicius MD. Dissociable intrinsic connectivity networks for salience processing and executive control. *J Neurosci Off J Soc Neurosci.* Feb; 2007 27(9):2349–2356.
14. Fox MD, Raichle ME. Spontaneous fluctuations in brain activity observed with functional magnetic resonance imaging. *Nat Rev Neurosci.* Sep; 2007 8(9):700–711. [PubMed: 17704812]
15. Smith SM, Fox PT, Miller KL, Glahn DC, Fox PM, Mackay CE, Filippini N, Watkins KE, Toro R, Laird AR, Beckmann CF. Correspondence of the brain's functional architecture during activation and rest. *Proc Natl Acad Sci.* Aug; 2009 106(31):13040–13045. [PubMed: 19620724]
16. Sämann PG, Tully C, Spoomaker VI, Wetter TC, Holsboer F, Wehrle R, Czisch M. Increased sleep pressure reduces resting state functional connectivity. *Magma N Y N.* Dec; 2010 23(5–6): 375–389.
17. Larson-Prior LJ, Zempel JM, Nolan TS, Prior FW, Snyder AZ, Raichle ME. Cortical network functional connectivity in the descent to sleep. *Proc Natl Acad Sci.* Mar; 2009 106(11):4489–4494. [PubMed: 19255447]
18. Mhuircheartaigh RN, Rosenorn-Lanng D, Wise R, Jbabdi S, Rogers R, Tracey I. Cortical and subcortical connectivity changes during decreasing levels of consciousness in humans: a functional magnetic resonance imaging study using propofol. *J Neurosci Off J Soc Neurosci.* Jul; 2010 30(27):9095–9102.
19. Pizoli CE, Shah MN, Snyder AZ, Shimony JS, Limbrick DD, Raichle ME, Schlaggar BL, Smyth MD. Resting-state activity in development and maintenance of normal brain function. *Proc Natl Acad Sci.* Jun.2011 :201109144.
20. Hutchison RM, Gallivan JP, Culham JC, Gati JS, Menon RS, Everling S. Functional connectivity of the frontal eye fields in humans and macaque monkeys investigated with resting-state fMRI. *J Neurophysiol.* May; 2012 107(9):2463–2474. [PubMed: 22298826]
21. Schwarz AJ, Gass N, Sartorius A, Risterucci C, Spedding M, Schenker E, Meyer-Lindenberg A, Weber-Fahr W. Anti-correlated cortical networks of intrinsic connectivity in the rat brain. *Brain Connect.* 2013; 3(5):503–511. [PubMed: 23919836]
22. Nasrallah FA, Tay HC, Chuang KH. Detection of functional connectivity in the resting mouse brain. *NeuroImage.* Feb.2014 86:417–424. [PubMed: 24157920]
23. Shulman GL, Fiez JA, Corbetta M, Buckner RL, Miezin FM, Raichle ME, Petersen SE. Common Blood Flow Changes across Visual Tasks: II. Decreases in Cerebral Cortex. *J Cogn Neurosci.* 1997; 9(5):648–663. [PubMed: 23965122]
24. Gusnard DA, Raichle ME, Raichle ME. Searching for a baseline: functional imaging and the resting human brain. *Nat Rev Neurosci.* Oct; 2001 2(10):685–694. [PubMed: 11584306]

25. Greicius MD, Krasnow B, Reiss AL, Menon V. Functional connectivity in the resting brain: a network analysis of the default mode hypothesis. *Proc Natl Acad Sci U S A*. Jan; 2003 100(1): 253–258. [PubMed: 12506194]
26. Beckmann CF, DeLuca M, Devlin JT, Smith SM. Investigations into resting-state connectivity using independent component analysis. *Philos Trans R Soc Lond B Biol Sci*. May; 2005 360(1457):1001–1013. [PubMed: 16087444]
27. De Luca M, Beckmann CF, De Stefano N, Matthews PM, Smith SM. fMRI resting state networks define distinct modes of long-distance interactions in the human brain. *NeuroImage*. Feb; 2006 29(4):1359–1367. [PubMed: 16260155]
28. Power JD, Cohen AL, Nelson SM, Wig GS, Barnes KA, Church JA, Vogel AC, Laumann TO, Miezin FM, Schlaggar BL, Petersen SE. Functional Network Organization of the Human Brain. *Neuron*. Nov; 2011 72(4):665–678. [PubMed: 22099467]
29. Yeo BTT, Krienen FM, Sepulcre J, Sabuncu MR, Lashkari D, Hollinshead M, Roffman JL, Smoller JW, Zollei L, Polimeni JR, Fischl B, Liu H, Buckner RL. The organization of the human cerebral cortex estimated by intrinsic functional connectivity. *J Neurophysiol*. Sep; 2011 106(3): 1125–1165. [PubMed: 21653723]
30. Damoiseaux JS, Rombouts SARB, Barkhof F, Scheltens P, Stam CJ, Smith SM, Beckmann CF. Consistent resting-state networks across healthy subjects. *Proc Natl Acad Sci U S A*. Sep; 2006 103(37):13848–13853. [PubMed: 16945915]
31. van den Heuvel M, Mandl R, Hulshoff Pol H. Normalized Cut Group Clustering of Resting-State fMRI Data. *PLoS ONE*. Apr.2008 3(4):e2001. [PubMed: 18431486]
32. Lee MH, Hacker CD, Snyder AZ, Corbetta M, Zhang D, Leuthardt EC, Shimony JS. Clustering of Resting State Networks. *PLoS ONE*. Jul.2012 7(7):e40370. [PubMed: 22792291]
33. Fox MD, Snyder AZ, Vincent JL, Corbetta M, Essen DCV, Raichle ME. The human brain is intrinsically organized into dynamic, anticorrelated functional networks. *Proc Natl Acad Sci U S A*. Jul; 2005 102(27):9673–9678. [PubMed: 15976020]
34. Golland Y, Golland P, Bentin S, Malach R. Data-driven clustering reveals a fundamental subdivision of the human cortex into two global systems. *Neuropsychologia*. Jan; 2008 46(2):540–553. [PubMed: 18037453]
35. Chai XJ, Castañón AN, Ongür D, Whitfield-Gabrieli S. Anticorrelations in resting state networks without global signal regression. *NeuroImage*. Jan; 2012 59(2):1420–1428. [PubMed: 21889994]
36. Zhang Z, Liao W, Zuo XN, Wang Z, Yuan C, Jiao Q, Chen H, Biswal BB, Lu G, Liu Y. Resting-State Brain Organization Revealed by Functional Covariance Networks. *PLoS ONE*. Dec.2011 6(12):e28817. [PubMed: 22174905]
37. Doucet G, Naveau M, Petit L, Delcroix N, Zago L, Crivello F, Jobard G, Tzourio-Mazoyer N, Mazoyer B, Mellet E, Joliot M. Brain activity at rest: a multiscale hierarchical functional organization. *J Neurophysiol*. Jun; 2011 105(6):2753–2763. [PubMed: 21430278]
38. Jack AI, Dawson AJ, Begany KL, Leckie RL, Barry KP, Ciccio AH, Snyder AZ. fMRI reveals reciprocal inhibition between social and physical cognitive domains. *NeuroImage*. Oct.2012 66C: 385–401. [PubMed: 23110882]
39. Spreng RN. The Fallacy of a ‘Task-Negative’ Network. *Front Psychol*. May.2012 3
40. Tomasi D, Volkow ND. Resting functional connectivity of language networks: characterization and reproducibility. *Mol Psychiatry*. Jul; 2012 17(8):841–854. [PubMed: 22212597]
41. Lee MH, Smyser CD, Shimony JS. Resting-state fMRI: a review of methods and clinical applications. *AJNR Am J Neuroradiol*. Oct; 2013 34(10):1866–1872. [PubMed: 22936095]
42. Hacker CD, Laumann TO, Szrama NP, Baldassarre A, Snyder AZ, Leuthardt EC, Corbetta M. Resting state network estimation in individual subjects. *NeuroImage*. Nov.2013 82:616–633. [PubMed: 23735260]
43. Corbetta M, Shulman GL. Control of goal-directed and stimulus-driven attention in the brain. *Nat Rev Neurosci*. Mar; 2002 3(3):201–215. [PubMed: 11994752]
44. Fox MD, Corbetta M, Snyder AZ, Vincent JL, Raichle ME. Spontaneous neuronal activity distinguishes human dorsal and ventral attention systems. *Proc Natl Acad Sci*. Jun; 2006 103(26): 10046–10051. [PubMed: 16788060]

45. Astafiev SV, Shulman GL, Corbetta M. Visuospatial reorienting signals in the human temporoparietal junction are independent of response selection. *Eur J Neurosci*. Jan; 2006 23(2):591–596. [PubMed: 16420468]
46. Vincent JL, Kahn I, Snyder AZ, Raichle ME, Buckner RL. Evidence for a frontoparietal control system revealed by intrinsic functional connectivity. *J Neurophysiol*. Dec; 2008 100(6):3328–3342. [PubMed: 18799601]
47. Power JD, Petersen SE. Control-related systems in the human brain. *Curr Opin Neurobiol*. Apr; 2013 23(2):223–228. [PubMed: 23347645]
48. Dosenbach NUF, Visscher KM, Palmer ED, Miezin FM, Wenger KK, Kang HC, Burgund ED, Grimes AL, Schlaggar BL, Petersen SE. A core system for the implementation of task sets. *Neuron*. Jun; 2006 50(5):799–812. [PubMed: 16731517]
49. Keles GE, Lamborn KR, Berger MS. Low-grade hemispheric gliomas in adults: a critical review of extent of resection as a factor influencing outcome. *J Neurosurg*. Nov; 2001 95(5):735–745. [PubMed: 11702861]
50. Keles GE, Chang EF, Lamborn KR, Tihan T, Chang CJ, Chang SM, Berger MS. Volumetric extent of resection and residual contrast enhancement on initial surgery as predictors of outcome in adult patients with hemispheric anaplastic astrocytoma. *J Neurosurg*. Jul; 2006 105(1):34–40. [PubMed: 16871879]
51. Lacroix M, Abi-Said D, Fournay DR, Gokaslan ZL, Shi W, DeMonte F, Lang FF, McCutcheon IE, Hassenbusch SJ, Holland E, Hess K, Michael C, Miller D, Sawaya R. A multivariate analysis of 416 patients with glioblastoma multiforme: prognosis, extent of resection, and survival. *J Neurosurg*. Aug; 2001 95(2):190–198. [PubMed: 11780887]
52. McGirt MJ, Chaichana KL, Gathinji M, Attenello FJ, Than K, Olivi A, Weingart JD, Brem H, Quiñones-Hinojosa AR. Independent association of extent of resection with survival in patients with malignant brain astrocytoma. *J Neurosurg*. Jan; 2009 110(1):156–162. [PubMed: 18847342]
53. Sanai N, Mirzadeh Z, Berger MS. Functional Outcome after Language Mapping for Glioma Resection. *N Engl J Med*. 2008; 358(1):18–27. [PubMed: 18172171]
54. Shimony JS, Zhang D, Johnston JM, Fox MD, Roy A, Leuthardt EC. Resting-state spontaneous fluctuations in brain activity: a new paradigm for presurgical planning using fMRI. *Acad Radiol*. May; 2009 16(5):578–583. [PubMed: 19345899]
55. Kokkonen SM, Nikkinen J, Remes J, Kantola J, Starck T, Haapea M, Tuominen J, Tervonen O, Kiviniemi V. Preoperative localization of the sensorimotor area using independent component analysis of resting-state fMRI. *Magn Reson Imaging*. Jul; 2009 27(6):733–740. [PubMed: 19110394]
56. Liu H, Buckner RL, Talukdar T, Tanaka N, Madsen JR, Stufflebeam SM. Task-free presurgical mapping using functional magnetic resonance imaging intrinsic activity. *J Neurosurg*. Oct; 2009 111(4):746–754. [PubMed: 19361264]
57. Stufflebeam SM, Liu H, Sepulcre J, Tanaka N, Buckner RL, Madsen JR. Localization of focal epileptic discharges using functional connectivity magnetic resonance imaging. *J Neurosurg*. Jun; 2011 114(6):1693–1697. [PubMed: 21351832]
58. Zhang X, Tokoglu F, Negishi M, Arora J, Winstanley S, Spencer DD, Constable RT. Social network theory applied to resting-state fMRI connectivity data in the identification of epilepsy networks with iterative feature selection. *J Neurosci Methods*. Jul; 2011 199(1):129–139. [PubMed: 21570425]
59. Bettus G, Bartolomei F, Confort-Gouny S, Guedj E, Chauvel P, Cozzzone PJ, Ranjeva JP, Guye M. Role of resting state functional connectivity MRI in presurgical investigation of mesial temporal lobe epilepsy. *J Neurol Neurosurg Psychiatry*. Oct; 2010 81(10):1147–1154. [PubMed: 20547611]
60. Weaver KE, Chaovalitwongse WA, Novotny EJ, Poliakov A, Grabowski TG, Ojemann JG. Local functional connectivity as a pre-surgical tool for seizure focus identification in non-lesion, focal epilepsy. *Front Neurol*. 2013; 4:43. [PubMed: 23641233]
61. Tie Y, Rigolo L, Norton IH, Huang RY, Wu W, Orringer D, Mukundan S Jr, Golby AJ. Defining language networks from resting-state fMRI for surgical planning--a feasibility study. *Hum Brain Mapp*. Mar; 2014 35(3):1018–1030. [PubMed: 23288627]

62. Shehzad Z, Kelly AMC, Reiss PT, Gee DG, Gotimer K, Uddin LQ, Lee SH, Margulies DS, Roy AK, Biswal BB, Petkova E, Castellanos FX, Milham MP. The resting brain: unconstrained yet reliable. *Cereb Cortex* N Y N 1991. Oct; 2009 19(10):2209–2229.
63. Fox MD, Zhang D, Snyder AZ, Raichle ME. The global signal and observed anticorrelated resting state brain networks. *J Neurophysiol*. Jun; 2009 101(6):3270–3283. [PubMed: 19339462]
64. Jo HJ, Saad ZS, Simmons WK, Milbury LA, Cox RW. Mapping sources of correlation in resting state FMRI, with artifact detection and removal. *NeuroImage*. Aug; 2010 52(2):571–582. [PubMed: 20420926]
65. Vincent JL, Snyder AZ, Fox MD, Shannon BJ, Andrews JR, Raichle ME, Buckner RL. Coherent spontaneous activity identifies a hippocampal-parietal memory network. *J Neurophysiol*. Dec; 2006 96(6):3517–3531. [PubMed: 16899645]
66. Rumelhart DE, Hinton GE, Williams RJ. Learning representations by back-propagating errors. *Nature*. Oct; 1986 323(6088):533–536.
67. Zhang D, Johnston JM, Fox MD, Leuthardt EC, Grubb RL, Chicoine MR, Smyth MD, Snyder AZ, Raichle ME, Shimony JS. Preoperative sensorimotor mapping in brain tumor patients using spontaneous fluctuations in neuronal activity imaged with functional magnetic resonance imaging: initial experience. *Neurosurgery*. Dec; 2009 65(6 Suppl):226–236. [PubMed: 19934999]
68. Fox MD, Snyder AZ, Zacks JM, Raichle ME. Coherent spontaneous activity accounts for trial-to-trial variability in human evoked brain responses. *Nat Neurosci*. Jan; 2006 9(1):23–25. [PubMed: 16341210]
69. Zacks JM, Braver TS, Sheridan MA, Donaldson DI, Snyder AZ, Ollinger JM, Buckner RL, Raichle ME. Human brain activity time-locked to perceptual event boundaries. *Nat Neurosci*. Jun; 2001 4(6):651–655. [PubMed: 11369948]
70. Mitchell TJ, Hacker CD, Breshears JD, Szrama NP, Sharma M, Bundy DT, Pahwa M, Corbetta M, Snyder AZ, Shimony JS, Leuthardt EC. A novel data-driven approach to preoperative mapping of functional cortex using resting-state functional magnetic resonance imaging. *Neurosurgery*. Dec; 2013 73(6):969–982. discussion 982–983. [PubMed: 24264234]
71. He BJ, Snyder AZ, Vincent JL, Epstein A, Shulman GL, Corbetta M. Breakdown of functional connectivity in frontoparietal networks underlies behavioral deficits in spatial neglect. *Neuron*. Mar; 2007 53(6):905–918. [PubMed: 17359924]
72. Hermes D, Miller KJ, Noordmans HJ, Vansteensel MJ, Ramsey NF. Automated electrocorticographic electrode localization on individually rendered brain surfaces. *J Neurosci Methods*. Jan; 2010 185(2):293–298. [PubMed: 19836416]

- rsfMRI is a promising technique for pre-surgical planning with the objective of decreasing morbidity while maximizing complete resection of pathological tissue. However, the methodology is still in early stages of development.
- Further research is necessary to make these tools more accurate and available in the operating room.
- Additional research is needed to explore the differences between rsfMRI and ECS mapping, and to better understand the consequences of disrupted RSNs outside the motor and language systems.
- Related engineering development should incorporate the pre-surgical MRI results into intra-operative neuro-navigation systems, including the rsfMRI results in conjunction with white matter fiber bundle anatomy derived from diffusion tensor imaging.

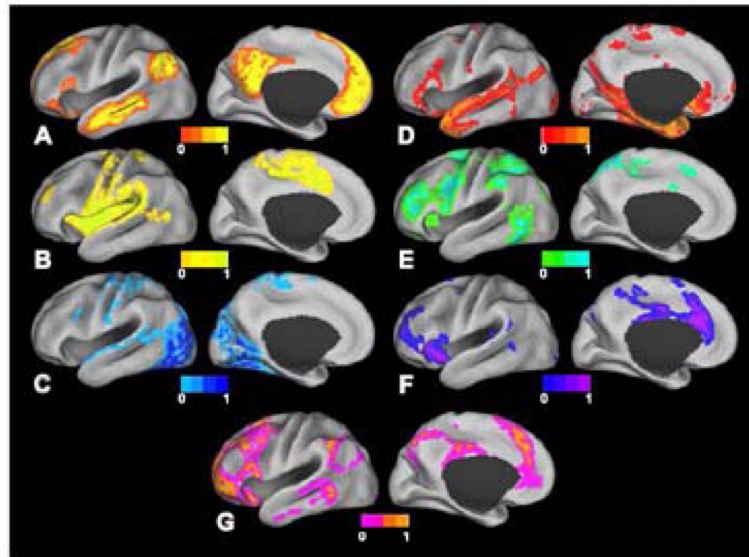


Figure 1. Surface plots of RSNs as derived from fuzzy c-means algorithm [32]. *A*: Default mode network. *B*: Somatomotor network. *C*: Visual network. *D*: Language network. *E*: Dorsal attention network. *F*: ventral attention network. *G*: Frontoparietal control network. Image from [32] used with permission.

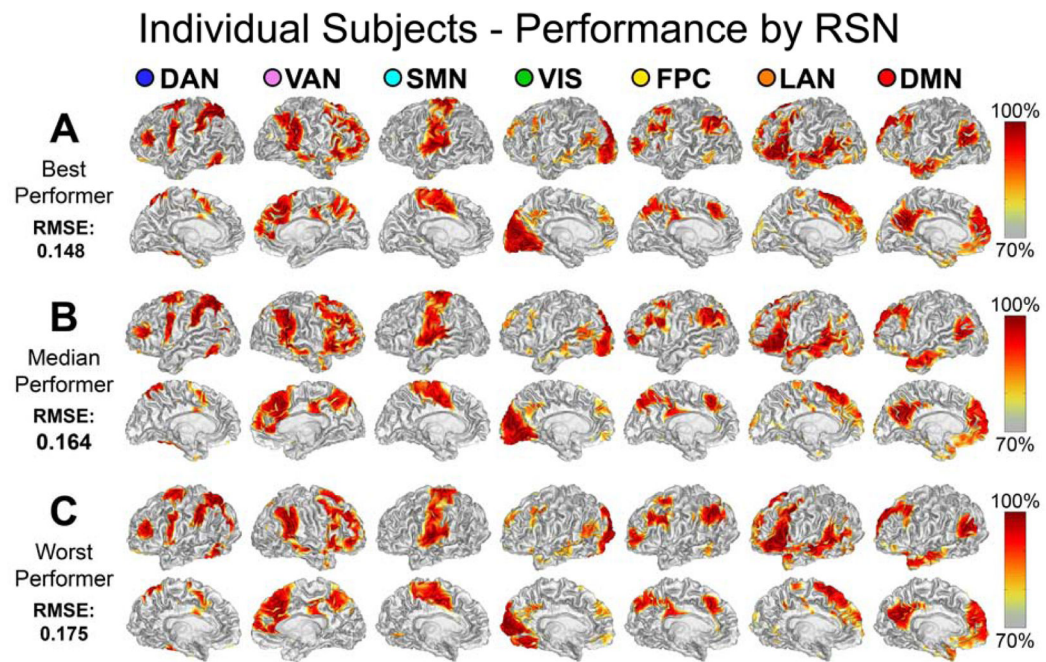


Figure 2.

Single subject, voxel estimation of RSNs using the trained MLP in three subjects. The results are from the best, median, and worst performers as determined by root mean square classification error. MLP output was converted to a percentile scale and sampled onto each subject's cortical surface. Image from [42] used with permission.

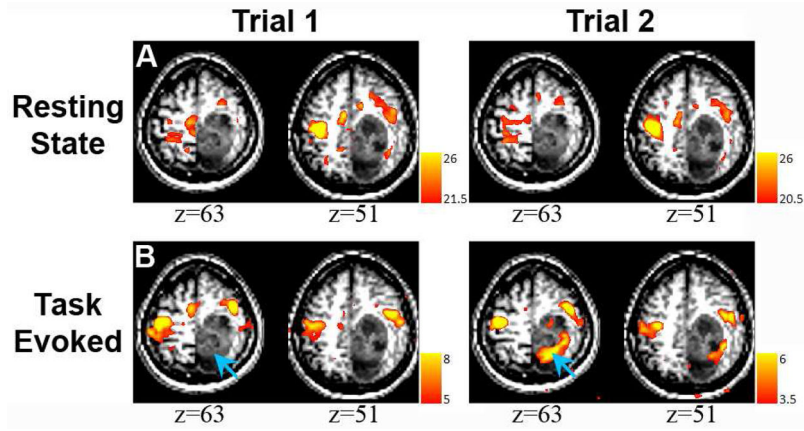


Figure 3. Comparison of resting state and task-related fMRI mapping in a 45 year old with a diagnosis of Glioblastoma (Case 1). A: Finger-tapping fMRI $\times 2$. Activity within the tumor (blue arrows) was seen in trial 2 but not in trial 1. B: Resting state correlation mapping $\times 2$ shows a similar distribution of correlated activity, resembling the activation from trial 1 but not trial 2. Image from [67] used with permission.

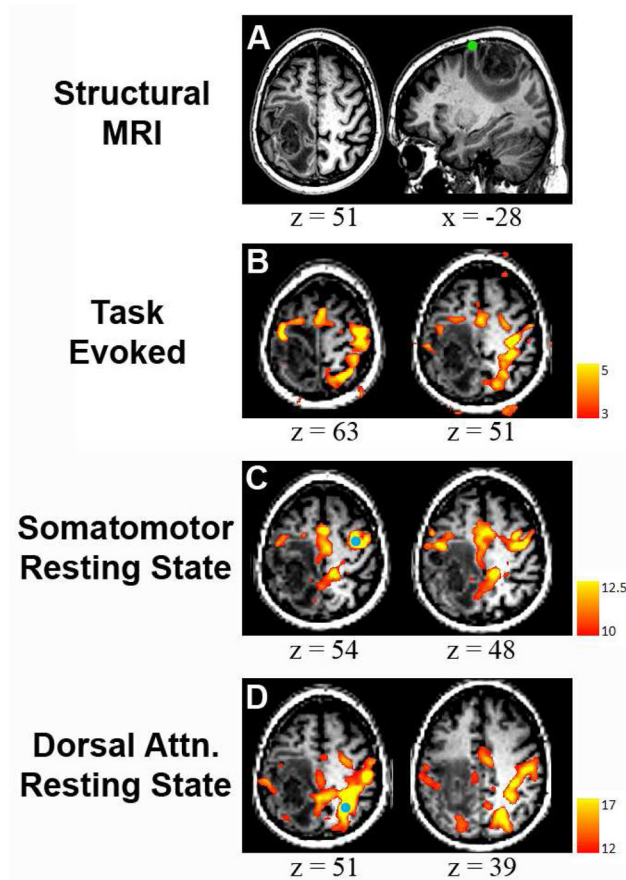


Figure 4.

MRI of a 64-year-old man who presented with focal motor seizures (Case 2). A: Structural MRI revealed a tumor in left parietal cortex that invades territory near the central sulcus (neurologic convention). The green circle represents the location of ipsilateral hand response to cortical stimulation. B: Task-related activity was seen bilaterally in frontal lobe. In addition, a large band of activity appeared in right parietal cortex, not consistent with the pattern of activity from the sensorimotor network. C: Resting state correlation mapping using a seed in the right (unaffected) hemisphere (blue circle) showed ipsilateral correlations anterior to the tumor as well as a region of activity in midline parietal cortex. Note absence in the correlation mapping results of parietal activity seen in the task-related map. D: Parietal activation seen during task-evoked scan is revealed to be a separate resting state network, the dorsal attention network that is normally dissociated from the sensorimotor network (seed: blue circle). Image from [67] used with permission.

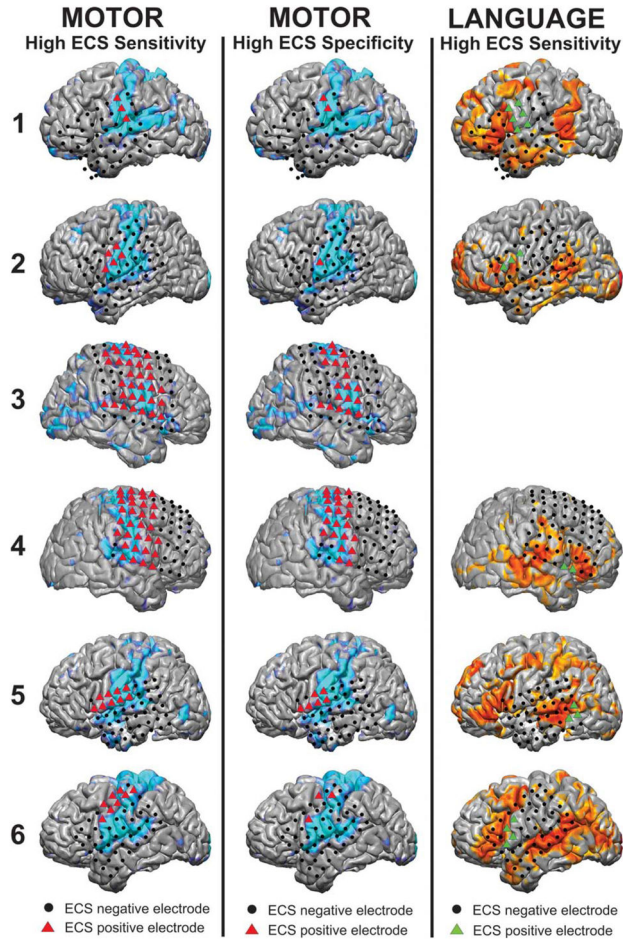


Figure 5. Comparison of ECS and MLP result for the motor and language cortex in six epilepsy patients. Colored triangles are ECS positive and Black circles are ECS negative. In the left column, the high ECS sensitivity method was employed to classify motor electrodes as ECS positive (red triangles) and compared to the MLP results (light blue). In the middle column, the high ECS specificity method was employed to classify motor electrodes. In the right column, the high ECS sensitive method was used to classify language electrodes as ECS positive (green triangles), with the MLP results displayed in orange. Image from [70] used with permission.

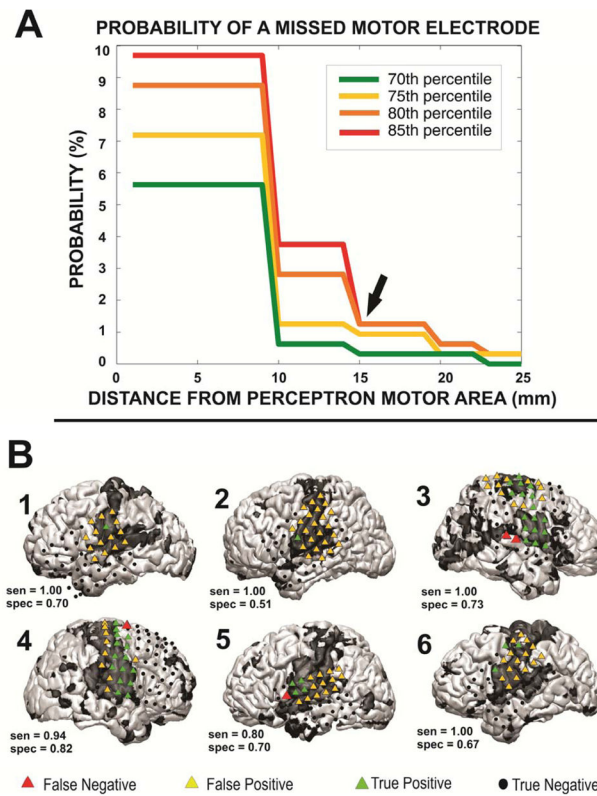


Figure 6.

The method employed to define a “no-cut” area in epilepsy patients, in which the probability of damage to motor cortex is substantial. A: To define the area, several multilayer perceptron (MLP) thresholds (70, 75, 80, 85 percentiles) were used to classify electrodes as covering motor cortex, and the “no-cut” zone was expanded around each of the motor electrodes. The probability of a missed motor electrode, which could result in motor deficits, was plotted against the radius of expansion. B: A visualization of the method performed at the 85% and at a radius of expansion of 15 mm. Red triangles mark motor cortex as determined by ECS that were missed by the MLP method. Image from [70] used with permission.

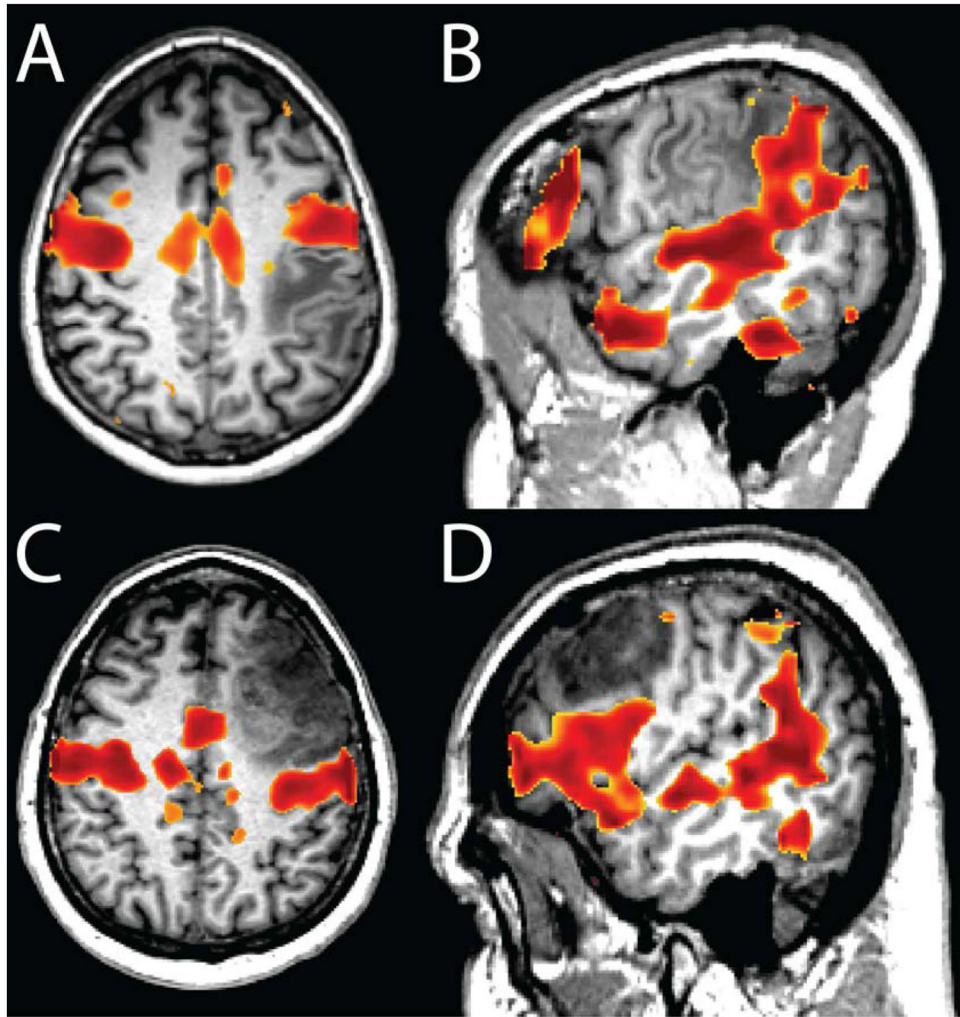


Figure 7. Examples of RSN (in red) superposed on T1-weighted images in two case examples. The somatomotor (A) and language (B) RSNs are shown for case example 1 (2.5.1). Similarly, the somatomotor (C) and language (D) RSNs are shown for case example 2 (2.5.2). See text for more detail.

Table 1

Task based fMRI	Resting state fMRI
<p>a. Neuronal activity is studied while performing a well-defined task, e.g., finger tapping or object naming.</p> <p>b. Task based fMRI maps a single functional system at a time.</p> <p>c. Task related changes in the blood oxygen level dependent (BOLD) signal are measured. Regions in the brain associated with a given task are localized.</p> <p>d. Task based fMRI is immune to spurious variance in the BOLD signal (e.g. pCO₂ levels, Head Motion).</p>	<p>a. Neuronal activity is studied in the absence of a task, i.e. when the subject in the scanner is in a state of quite wakefulness.</p> <p>b. rsfMRI maps all functional systems simultaneously.</p> <p>c. Spontaneous fluctuations in the BOLD signal are measured. Correlated intrinsic activity defines functional connectivity.</p> <p>d. rsfMRI is vulnerable to contamination and requires denoising to remove sources of spurious variance.</p>

Table 2

Resting state fMRI networks	
1. <i>Default Mode Network (DMN)</i>	Most robust resting state network More active at rest than during performance of goal-directed tasks
2. <i>Somatomotor Network (SMN)</i>	Includes primary and higher order motor and sensory areas
3. <i>Auditory Network</i>	Includes Heschl's gyrus, superior temporal gyrus, and posterior insula
4. <i>Visual Network</i>	Includes most of the occipital cortex
5. <i>Language Network</i>	Includes Broca's, Wernicke's and multiple other language related areas Extends to prefrontal, temporal, parietal, and subcortical regions
6. <i>Dorsal Attention Network (DAN)</i>	Tasks requiring spatial attention Includes intraparietal sulcus and frontal eye field
7. <i>Ventral Attention Network (VAN)</i>	Involved in detection of environmentally salient events Includes temporal-parietal junction
8. <i>Frontoparietal Control Network</i>	Associated with working memory and control of goal-directed behavior Includes lateral prefrontal cortex and inferior parietal lobule
9. <i>Cingulo-opercular Network (CON)</i>	Associated with performance of tasks requiring executive control Medial superior frontal and anterior prefrontal cortices, anterior insula

Table 3

Resting state fMRI and pre-surgical planning	
1	rsfMRI can be performed in patients who may not be able to complete task-based paradigms e.g. young children, uncooperative patients, and patients who are sedated, paretic, or aphasic. Provides a map of resting state architecture including multiple RSNs of the brain prior to surgery. In patients with brain tumors this is particularly valuable when intraoperative electro-cortical stimulation cannot be performed.
2	Identifies multiple networks simultaneously, saving time when information on multiple networks may be required.
3	The topography of RSNs closely corresponds to the topography elicited by task fMRI.
4	RSNs are generally symmetric, thus determining language lateralization is more challenging than in task based fMRI and is an area of active research.
